

*Technical Supplement of*

5 **Estimations of statistical dependence as joint return period modulator  
of compound events. Part I: storm surge and wave height.**

Thomas I. Petroligkis

Correspondence to: Thomas I. Petroligkis ([thomas.petroligkis@ec.europa.eu](mailto:thomas.petroligkis@ec.europa.eu))

10

15 ***Contents***

*S1 Details of RIEN (RIver ENding) point positions*

*S2 Additional validation of wave hindcasts (focusing on extremes)*

20

*S3 Capability of storm surge and wave hindcasts to identify and resolve compound events*

*S4 Analytical values of correlation and statistical dependence based on Matlab routines*

25 *S5 Analytical values of correlation and statistical dependence based mainly on R routines*

*S6 References*

30

35

S1 Details of RIEN (RIVER ENDing) point positions

The current statistical (dependence) analysis is focused over 32 river ending points that have been selected to cover a variety of riverine and estuary areas along European coasts. The sea areas used in the study refer to the Mediterranean Sea (central and north Adriatic Sea, Balearic Sea, Alboran Sea and Gulf of Lion), West Iberian, North Iberian, Bay of Biscay, Irish Sea, Bristol Channel, English Channel, North Sea, Norwegian Sea, Baltic Sea and Black Sea. A map showing the position of RIEN (RIVER ENDing) points used in the study is shown in Fig. 1 of the main text. Additional details can be found in Table S1 (current Technical Supplement) containing the exact location (lat, lon) of all RIEN points

Table S1. Positions (lat, lon) of 32 RIEN points used in the study. Names refer to river ending areas.

	RIEN	lat	lon		RIEN	lat	lon
1	Po Della Pila	44.96	12.49	17	Muir Eireann	52.65	-6.22
2	Madonna Del Ponte	43.83	13.05	18	Wallasey	53.44	-3.04
3	Martinsicuro	42.84	13.93	19	Severn Bridge	51.61	-2.65
4	Aries	43.34	4.84	20	Fort Picklecombe	50.34	-4.17
5	El Foix	41.20	1.67	21	Exmouth	50.62	-3.42
6	Illa de Buda	40.71	0.89	22	Christchurch District	50.72	-1.74
7	Rio De Velez	36.72	-4.11	23	Dieppe	49.91	1.09
8	Matosinhos	41.18	-8.71	24	South Tynesid	55.01	-1.43
9	Carcavelos	38.69	-9.26	25	Spurm Point	53.57	0.11
10	Setubal	38.53	-8.89	26	Sheerness	51.45	0.74
11	San Bruno	37.18	-7.39	27	Western Scheldt	51.43	3.55
12	Punta Del Arenal	43.47	-5.07	28	Rockanje	51.87	4.01
13	Concarneau	47.86	-3.92	29	Wurster Arm	53.65	8.14
14	Riviere De Belon	47.81	-3.72	30	Kattegat	57.77	11.76
15	Larmor-Plage	47.71	-3.38	31	Trondheimsfjord	63.32	9.82
16	Musura Bay	45.22	29.73	32	Vanhankaupunginselka	60.24	24.99

**S2 Additional validation of wave hindcasts (focusing on extremes)**

The set of storm surge hindcasts originated from Vousdoukas et al. (2016) have specifically used for projections of extreme storm surge levels along Europe and it seems as an appropriate dataset for the current paper. On the other hand, wave hindcasts based on the ERA5 significant wave reanalysis dataset have not been thoroughly tested as for the validity of their extreme values since ERA5 has been in production phase (<https://www.ecmwf.int/en/about/media-centre/science-blog/2017/era5-new-reanalysis-weather-and-climate-data>).

Due to this (limitation), an investigation was performed over a set of 13 wave buoys along European coasts capable of providing enough hourly data for such an analysis. The details of wave buoys used are shown in Table S2. Buoys over Mediterranean are denoted as MED, over Bay of Biscay as BIS, over Irish Sea as IRI and over North Sea as NOS. HvH-LiG refers to the wave buoy Lightland Goeree stationed near the coastal area of Hook van Holland (NL).

**Table S2.** Details of wave buoys used in the validation of wave extremes.

	id	name	lat	lon	days	corr
M	61217	Adriatic Sea	42.41	14.54	203	0.94
E	61218	Adriatic Sea	43.83	13.72	1,588	0.87
D	61280	Balearic Sea	40.69	1.48	2,764	0.87
B I S	62001	Bay of Biscay	45.20	-5.00	6,012	0.97
I R I	62091	Irish Sea	53.48	-5.43	4,991	0.93
	62094	Irish Sea	51.70	-6.70	3,727	0.94
	62301	Irish Sea	52.40	-4.70	5,339	0.93
	62303	Bristol Channel	51.50	-5.10	7,426	0.94
N O S	62127	North Sea	54.00	0.70	1,158	0.92
	62142	North Sea	53.00	2.10	5,537	0.92
	62145	North Sea	53.10	2.80	5,796	0.92
	63115	North Sea	61.60	1.30	2,922	0.97
	HvH-LiG	North Sea	51.93	3.40	1,114	0.92

Based on these 13 wave buoys listed in Table S2, a dataset of 48,547 pairs of daily maxima was compiled comprising hindcast and observation values. The mean error (bias) of hindcasts was found to be equal to -0.29 m with a corresponding rmse of 0.56 m. From a closer investigation, it became obvious that there were cases with hindcasts not capturing the exact magnitude of extremes. In such cases emphasis was given to the possibility of capturing (resolving) the extremes as spikes, i.e., as “footprints” of extreme values.

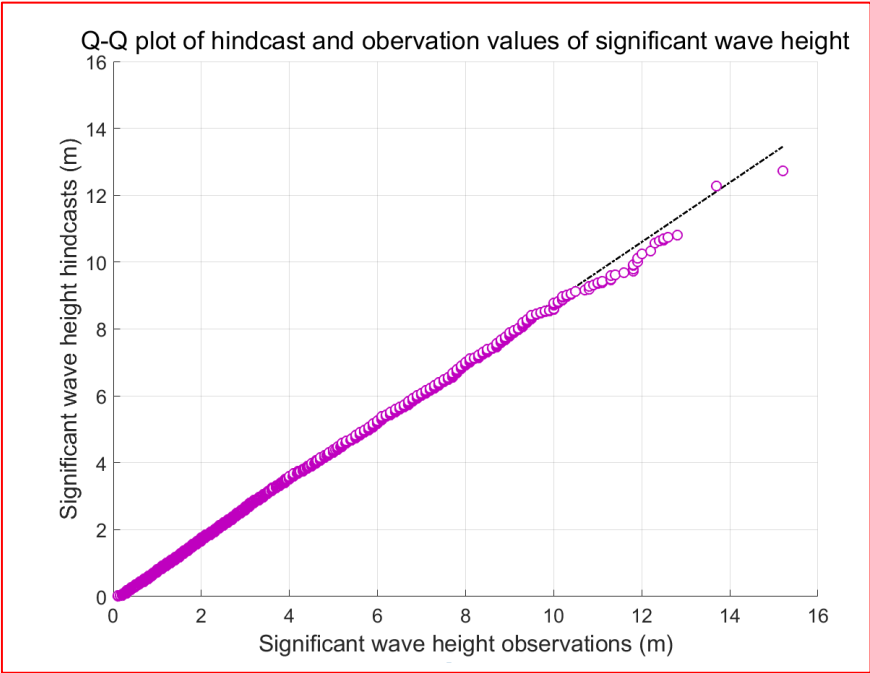


**Figure S1.** Q-Q (quantile-quantile) plot of hindcast and observation values of significant wave height.

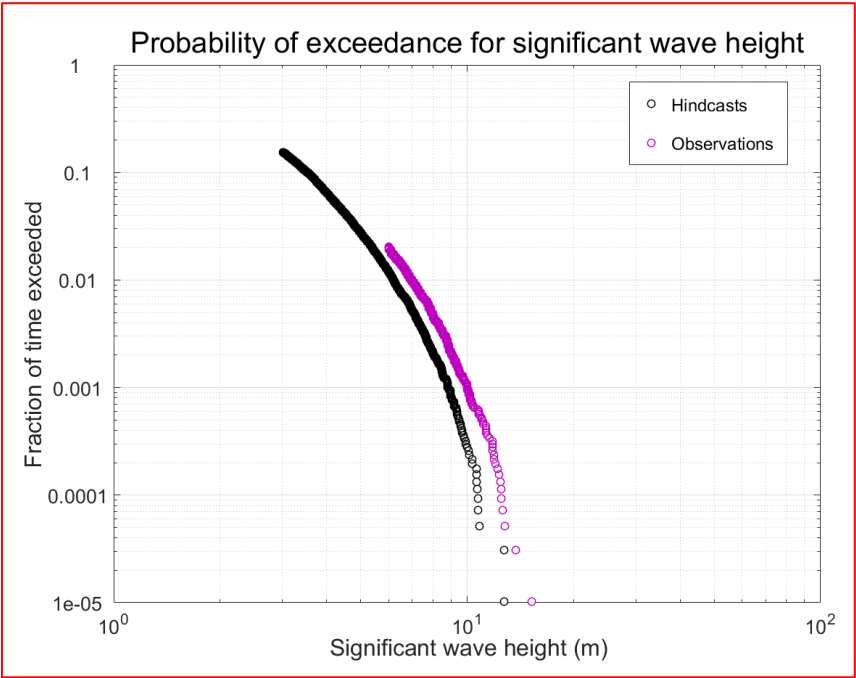


**Figure S2.** PoE (Probability of Exceedance) for wave observations (red color) and hindcasts (blue color).

In addition, both Fig. S1 (Quantile-Quantile Plot) and Fig. S2 (Probability of Exceedance Plot) seem to support this unavoidable limitation since due to the low resolution models used for reproducing time series of significant weather parameters (as in this case), extremes cannot be captured with their exact (high-impact) value but in most cases their “footprint” signal can be resolved as a spike of a lesser value. A relevant example can be seen in Petroliaġis and Pinson (2012) where the footprints of extreme wind speed values over Bremen airport are captured by ERA-Interim as footprint spikes although significantly underestimated (compared to observations) but still capable of resolving extremes as shown in Figure 7 of Petroliaġis & Pinson.

**Table S3.** Number of hits for various hindcast and observation thresholds (percentiles).

thrs	hind	obs	events	hits	score
55	1.51	1.80	6,617	6,129	93 %
60	1.81	2.10	5,673	5,135	91 %
65	1.97	2.30	5,041	4,586	91 %
70	2.17	2.50	4,506	4,023	89 %
75	2.41	2.80	3,737	3,329	89 %
80	2.69	3.05	3,281	2,821	86 %
85	3.05	3.40	2,527	2,147	85 %
90	3.53	4.00	1,699	1,439	85 %
91	3.65	4.10	1,586	1,314	83 %
92	3.77	4.30	1,394	1,159	83 %
93	3.91	4.50	1,243	1,033	83 %
94	4.08	4.70	1,070	881	83 %
95	4.29	4.90	948	768	81 %
96	4.56	5.20	775	620	80 %
97	4.89	5.60	601	479	80 %
98	5.38	6.20	417	337	81 %
99	6.18	7.20	233	186	80 %

In a similar way, during the estimation of statistical dependence such footprints seem to be capable of determining the days of the most extreme wave daily maxima. The main issue in estimating dependence is not the exact magnitude of extremes (i.e., how well are resolved by hindcasts) but rather if a spike (footprint of an extreme) exists on a specific day denoting the exceedance over a critical percentile threshold of hindcasts. If such (correct) footprint is considered as a hit, Table S3 was  
5 compiled containing the number of hits over a set of critical (hindcast & observation) wave thresholds in a POT (Peaks Over Threshold) environment.

Taking into consideration that during the estimation of dependence (Table S6 and Table S7 of Technical Supplement), threshold (percentile) wave values ranging from 86.2 to 98.8% were used, this corresponds to 80 to 85% hits (i.e., correct  
10 footprint spikes of daily maxima denoting an extreme).

Lastly, in cases of **compound (surge & wave)** footprints of extremes (resolved by hindcasts), Table S4 (Technical Supplement) has been compiled where the 98.5% percentile extremes of storm surge observations are compared to their corresponding hindcast values (falling in the same 98.5% category). Same way in Table S5 (Technical Supplement), the  
15 footprints of significant wave height observation extremes are compared to their corresponding hindcast (or lesser intensity) values.

It becomes obvious that although hindcasts could not resolve the exact extremity of both surge and wave events, they were able to capture their footprints quite well. It is important to point out that hindcasts above all were capable of identifying and  
20 resolving all seven (7) compound events that took place during the common time interval of 1,114 days referring to the RIEN point of Rhine River.

**S3 Capability of storm surge and wave hindcasts to identify and resolve compound events**

As already mentioned long-period water level data coinciding with wave observations directly or very close to the exact sites of interest (RIEN points) were not available with the exception of the Rhine River (RIEN). For this RIEN, concurrent (close-  
5 by) observations with no gaps of sea level, astronomical tide, storm surge, and wave height from a close-by wave buoy were available for a period of about 3 years (1,114 days).

In Table S4, extreme storm surge (above 98.5% percentile) values for both observations in red and hindcasts for HvH tide gauge station over the common time interval of 1,114 days are shown. Same way extreme significant wave height (above  
10 98.5% percentile) values for both observations and hindcasts for LiG wave buoy station over the common time interval are contained in Table S5.

**Table S4.** Extreme storm surge (above 98.5% percentile) values for observations in red (>0.95m) and hindcasts (>0.89m) for  
HvH tide gauge station over the common time interval of 1,114 days. Compound events of surge and wave (i.e., both surge  
15 & wave above critical threshold) are marked by orange shade.

#	Date	Observations	hindcasts
1	12 Nov 2010	1.38	1.10
2	4 Feb 2011	1.20	1.00
3	27 Nov 2011	1.25	1.04
4	28 Nov 2011	0.98	0.93
5	3 Dec 2011	1.08	1.03
6	7 Dec 2011	1.10	0.95
7	9 Dec 2011	1.45	1.23
8	29 Dec 2011	1.23	1.03
9	3 Jan 2012	1.07	0.47
10	4 Jan 2012	1.46	1.16
11	5 Jan 2012	1.66	1.59
12	6 Jan 2012	1.37	1.57
13	21 Jan 2012	1.09	1.02
14	22 Jan 2012	1.00	1.07
15	30 Jan 2013	1.07	0.73
16	10 Sep 2013	0.96	0.59

Compound events of surge and wave are marked by orange shade (in both Table S4 and Table S5) based on joint observations of storm surge and significant wave height. It becomes obvious that hindcasts were able to resolve all seven (7) compound events that took place during the common time period of 1,114 days.

5

**Table S5.** Extreme wave height (above 98.5% percentile) values for observations in red (> 4.07m) and hindcasts (>3.38m) for LiG wave buoy station over the common time interval of 1,114 days. Compound events of surge and wave (i.e., both surge & wave above critical threshold) are marked by orange shade.

#	Date	Observations	hindcasts
1	12 Nov 2010	4.79	3.99
2	14 Jul 2011	4.61	3.34
3	7 Oct 2011	4.34	3.34
4	7 Dec 2011	5.06	4.83
5	8 Dec 2011	4.49	3.87
6	9 Dec 2011	4.17	3.53
7	24 Dec 2011	4.37	3.27
8	29 Dec 2011	4.18	3.46
9	30 Dec 2011	4.66	3.84
10	4 Jan 2012	4.31	4.02
11	5 Jan 2012	5.14	4.79
12	6 Jan 2012	4.55	4.90
13	20 Jan 2012	4.15	2.81
14	31 Aug 2012	4.11	3.24
15	24 Sep 2012	4.61	3.43
16	25 Nov 2012	4.36	4.09

10 Further, an extra investigation based on extreme values of observations (during the common time interval of 1,114 days) exceeding a variety of percentile values (for the RIEN point of Rhine River) showed that both storm surge and their corresponding wave height hindcasts were able to capture almost all of the 24-hour extremes on the same (correct) day but with a weaker intensity (i.e., with a correct footprint of lesser intensity).

**S4 Analytical values of correlation and statistical dependence based on Matlab routines**

A necessary split of results had to be made for a better and easier visualisation due to the relatively large amount of RIEN points to fit in one single Table. This split also revealed the distinct differences between southern and northern coastal European areas. Details of both correlations and dependencies found over southern and northern RIEN points are presented analytically in Table S6 and Table S7 based on Matlab routines. Correlation (corr) and dependence (chi) values for both max12 and max24 intervals are presented together with critical threshold (thrs), significance (sig) and 95% confidence level (lower & upper) max24 values. Referring to correlation values, a large amount of variability is evident in both max12 and max24 modes

**Table S6.** Correlation and statistical dependence values for storm surge and significant wave heights over Mediterranean (ADR: Adriatic Sea – GOL: Gulf of Lion – BAL: Balearic Sea – ALB: Alboran Sea), West and North Iberian coasts (WIB & NIB), Bay of Biscay (BOB) and Black Sea (BLK) based on Matlab routines.

			max12			max24						
	RIEN	sea	corr	thrs	chi	corr	thrs	chi	chibar	sig	lower	upper
1	Po	ADR	0.26	97.4	0.28	0.39	97.1	0.29	0.43	0.02	0.21	0.37
2	Metauro	ADR	0.23	96.8	0.26	0.35	95.7	0.22	0.30	0.05	0.03	0.35
3	Vibrata	ADR	0.23	96.6	0.35	0.37	96.5	0.32	0.36	0.04	0.23	0.37
4	Rhone	GOL	0.08	94.6	0.20	0.13	93.8	0.21	0.17	0.04	0.13	0.30
5	Foix	BAL	0.09	92.2	0.03	0.10	91.2	0.03	0.05	0.03	0.00	0.08
6	Ebro	BAL	0.04	94.7	0.19	0.12	94.5	0.22	0.22	0.03	0.10	0.30
7	Velez	ALB	0.02	93.9	0.19	0.06	93.1	0.11	0.13	0.04	0.05	0.17
8	Douro	WIB	-0.18	97.0	0.30	-0.06	95.7	0.30	0.30	0.05	0.11	0.38
9	Tagus	WIB	-0.30	94.3	0.05	-0.22	93.7	0.14	0.16	0.03	0.09	0.22
10	Sado	WIB	-0.26	94.9	0.10	-0.19	93.9	0.13	0.17	0.03	0.06	0.21
11	Guadiana	WIB	-0.04	95.9	0.22	0.03	95.7	0.28	0.29	0.02	0.15	0.36
12	Sella	NIB	-0.25	93.2	0.10	-0.17	86.2	0.14	0.07	0.05	0.07	0.19
13	Moros	BOB	0.07	96.2	0.32	0.22	96.2	0.30	0.34	0.03	0.17	0.39
14	Aven	BOB	0.13	97.0	0.34	0.25	96.7	0.35	0.39	0.01	0.23	0.42
15	Blavet	BOB	0.11	96.5	0.33	0.25	96.7	0.34	0.39	0.02	0.22	0.40
16	Danube	BLK	-0.01	96.7	0.21	0.09	96.3	0.24	0.35	0.05	0.07	0.38

**Table S7.** As in Table S6 but for Irish Sea (IRS), Bristol Channel (BRC), English Channel (ENC), North Sea (NRS), Norwegian Sea (NOS) and Baltic Sea (BAS). Owena stands for Owenavarragh RIEN (IE) while Goeta is Goeta Aelv RIEN (ES).

			max12			max24						
	RIEN	sea	corr	thrs	chi	corr	thrs	chi	chibar	sig	lower	upper
17	Owena	IRS	0.50	98.4	0.46	0.59	97.9	0.45	0.53	0.05	0.30	0.55
18	Mersey	IRS	0.45	98.2	0.43	0.56	97.4	0.43	0.48	0.03	0.29	0.52
19	Severn	BRC	0.19	96.1	0.29	0.30	94.9	0.30	0.24	0.04	0.22	0.35
20	Tamar	ENC	0.28	97.8	0.35	0.39	96.9	0.35	0.41	0.02	0.24	0.49
21	Exe	ENC	0.31	97.9	0.38	0.41	97.1	0.40	0.43	0.03	0.29	0.54
22	Avon	ENC	0.37	98.1	0.44	0.50	97.9	0.48	0.55	0.04	0.35	0.58
23	Bethune	ENC	0.59	99.1	0.62	0.68	98.8	0.64	0.77	0.02	0.55	0.73
24	Tyne	NRS	0.14	91.7	0.31	0.28	94.5	0.26	0.21	0.05	0.10	0.39
25	Humber	NRS	0.18	97.3	0.35	0.38	96.6	0.35	0.37	0.04	0.20	0.49
26	Thames	NRS	-0.10	92.6	0.22	0.06	92.7	0.22	0.11	0.05	0.11	0.31
27	Schelde	NRS	0.31	97.6	0.54	0.54	97.5	0.53	0.50	0.01	0.45	0.61
28	Rhine	NRS	0.52	98.5	0.57	0.67	98.0	0.56	0.57	0.03	0.41	0.64
29	Weser	NRS	0.56	99.0	0.58	0.65	98.5	0.56	0.69	0.02	0.42	0.63
30	Goeta	NRS	0.43	97.2	0.53	0.55	96.8	0.51	0.39	0.05	0.44	0.61
31	Orkla	NOS	0.35	97.6	0.46	0.46	97.0	0.41	0.43	0.03	0.33	0.50
32	Vantaa	BAS	0.30	97.0	0.43	0.44	96.9	0.44	0.42	0.03	0.36	0.50

**S5 Analytical values of correlation and statistical dependence based mainly on R routines**

Details of both correlations and dependencies found over southern and northern RIEN points are presented analytically in Table S8 and Table S9 based mainly on R routines.

**Table S8.** As in Table S6, but based mainly on R (chiplot & taildep) routines. Ensemble mean (comb) values of dependence are also shown (last column).

5

			R				MAT	ENS
	RIEN	sea	lower	upper	chiplot	taildep	mat_chi	comb
1	Po	ADR	0.13	0.34	0.23	0.27	0.29	0.26
2	Metauro	ADR	0.08	0.26	0.17	0.22	0.22	0.20
3	Vibrata	ADR	0.13	0.32	0.23	0.36	0.32	0.30
4	Rhone	GOL	0.06	0.21	0.14	0.22	0.21	0.19
5	Foix	BAL	0.01	0.13	0.07	0.16	0.03	0.09
6	Ebro	BAL	0.14	0.30	0.22	0.28	0.22	0.24
7	Velez	ALB	0.03	0.18	0.10	0.16	0.11	0.12
8	Douro	WIB	0.17	0.33	0.26	0.31	0.30	0.29
9	Tagus	WIB	0.07	0.21	0.14	0.22	0.14	0.17
10	Sado	WIB	0.08	0.21	0.14	0.21	0.13	0.17
11	Guadiana	WIB	0.19	0.34	0.27	0.32	0.28	0.29
12	Sella	NIB	0.05	0.19	0.12	0.18	0.14	0.15
13	Moros	BOB	0.14	0.32	0.23	0.28	0.30	0.27
14	Aven	BOB	0.18	0.37	0.27	0.31	0.35	0.31
15	Blavet	BOB	0.17	0.36	0.27	0.30	0.34	0.30
16	Danube	BLK	0.13	0.32	0.23	0.26	0.24	0.24

**Table S9.** As in Table S7, but based mainly on R (chiplot & taildep) routines. Ensemble mean (comb) values of dependence are also shown (last column).

			R				MAT	ENS
	RIEN	sea	lower	upper	chiplot	taildep	mat_chi	comb
17	Owena	IRS	0.26	0.52	0.39	0.40	0.45	0.41
18	Mersey	IRS	0.26	0.48	0.38	0.38	0.43	0.40
19	Severn	BRC	0.16	0.32	0.24	0.30	0.30	0.28
20	Tamar	ENC	0.21	0.41	0.31	0.34	0.35	0.33
21	Exe	ENC	0.25	0.46	0.36	0.38	0.40	0.38
22	Avon	ENC	0.33	0.57	0.45	0.46	0.48	0.46
23	Bethune	ENC	0.49	0.80	0.64	0.66	0.64	0.65
24	Tyne	NRS	0.11	0.27	0.19	0.26	0.26	0.24
25	Humber	NRS	0.20	0.40	0.30	0.33	0.35	0.33
26	Thames	NRS	0.08	0.22	0.15	0.25	0.22	0.21
27	Schelde	NRS	0.36	0.58	0.47	0.48	0.53	0.49
28	Rhine	NRS	0.41	0.64	0.52	0.54	0.56	0.54
29	Weser	NRS	0.40	0.67	0.55	0.54	0.56	0.55
30	Goeta	NRS	0.35	0.53	0.44	0.46	0.51	0.47
31	Orkla	NOS	0.25	0.45	0.35	0.38	0.41	0.38
32	Vantaa	BAS	0.27	0.48	0.37	0.40	0.44	0.40

For the analysis of results, the ensemble mean value of  $\chi$  (by averaging mat\_chi, chiplot and taildep values) is taken as a reference value (contained in the last column of Table S8 and Table S9). The different categories of correlation and dependence used in the main text (and in Fig. 10) refers to the categorisation adapted by Defra TR1 Report (2005) and TR3 Report (2005).

## S6 References

- Defra TR1 Report by Hawkes, P.J. and Svensson, C.: Joint probability: dependence mapping & best practice. R & D Final Technical Report FD2308/TR1 to Defra. HR Wallingford and CEH Wallingford, U.K. ([http://evidence.environment-agency.gov.uk/FCERM/Libraries/FCERM\\_Project\\_Documents/FD2308\\_3428\\_TRP\\_pdf.sflb.ashx](http://evidence.environment-agency.gov.uk/FCERM/Libraries/FCERM_Project_Documents/FD2308_3428_TRP_pdf.sflb.ashx)), 2005.
- 5 Defra TR3 Report by Svensson, C. and Jones, D.A.: Joint Probability: Dependence between extreme sea surge, river flow and precipitation: a study in south and west Britain. Defra/Environment Agency R & D Technical Report FD2308/TR3, 62 pp. + appendices ([http://evidence.environment-agency.gov.uk/FCERM/Libraries/FCERM\\_Project\\_Documents/FD2308\\_3430\\_TRP\\_pdf.sflb.ashx](http://evidence.environment-agency.gov.uk/FCERM/Libraries/FCERM_Project_Documents/FD2308_3430_TRP_pdf.sflb.ashx)), 2005.
- Petroligis, T.I. and P. Pinson, 2014. Early warnings of extreme winds using the ECMWF Extreme Forecast Index. Meteorological Applications, 21, 171–185. DOI: 10.1002/met.1339.
- 10